

## Activity Difference between $\alpha$ -COOH and $\beta$ -COOH in *N*-Phosphorylaspartic Acids

Zhong-Zhou Chen, Bo Tan, Yan-Mei Li,\* and Yu-Fen Zhao

Key Laboratory for Bioorganic Phosphorus Chemistry of Education Ministry, Department of Chemistry, Tsinghua University, Beijing 100084, P. R. China

Yu-Feng Tong and Jin-Feng Wang

Center for Molecular Biology, National Laboratory of Biomacromolecules, Institute of Biophysics, Academia Sinica, 15 Datun Road, Beijing 100101, P. R. China

liym@mail.tsinghua.edu.cn

Received January 9, 2003

*N*-phosphorylamino acids are chemically active species that have many biomimic activities.  $\alpha$ -COOH in amino acids and peptides behaves rather differently than  $\beta$ -COOH in many biochemical processes and takes a more important role in the origin of life. Activity differences between  $\alpha$ -COOH and  $\beta$ -COOH in the peptide formation of phosphoryl amino acids are studied by 1D, 2D NMR techniques and by ab initio and density functional theory (DFT) calculations in this paper. Phosphoryl dipeptide is formed directly from phosphoryl aspartic acids without any coupling reagents. Only the  $\alpha$ -dipeptide ester is observed by 1D  $^1\text{H}$ ,  $^{13}\text{C}$ , and  $^{31}\text{P}$  NMR and 2D NMR. In the ab initio and DFT calculations, the pentacoordinate phosphorane intermediates containing five-membered rings are predicted to be more favored than those with six-membered rings. Both the experimental results and the theoretical calculations suggest that only the  $\alpha$ -COOH group is activated by *N*-phosphorylation in *N*-phosphorylaspartic acid under mild conditions.

### 1. Introduction

The difference between  $\alpha$ -amino acids and  $\beta$ -amino acids is of great importance in many biological processes. In the biosynthesis of peptides and proteins, only  $\alpha$ -amino acids are activated and incorporated. Recently,  $\beta$ -peptides, i.e., oligomers of  $\beta$ -amino acids, were found to form helix and  $\beta$ -sheet secondary structures,<sup>1</sup> which previously were considered to occur only for  $\alpha$ -peptides. The authors speculate that with properly arranged functional groups and various secondary and tertiary structures, large, complex  $\beta$ -peptides may bear protein-like active sites and enzymatic properties. These results make the question of "why nature chooses  $\alpha$ -amino acids, other than  $\beta$ -amino acids, in the biosynthesis of peptides and proteins" more amusing. Nonenzymatic deamidation of peptides and proteins represents an important degradation reaction occurring *in vitro* in the course of isolation or storage and *in vivo* during the development or aging of cells.<sup>2</sup> One of the particularly important results is the formation of  $\beta$ -peptide linkages, i.e., peptide bonds formed between  $\beta$ -COOH and  $-\text{NH}_2$  groups, after the deamidation of Asn, which might cause such diseases as epilepsy and Alzheimer's syndrome.<sup>3</sup> Moreover,  $\beta$ -peptide linkages are more

favored than the corresponding  $\alpha$ -peptide linkages in alkaline and neutral conditions.<sup>4</sup> Thus, it is important to probe the activity difference between  $\alpha$ -COOH and  $\beta$ -COOH to gain further insights into diseases related to  $\beta$ -peptide linkages.

Many biological processes are regulated by the phosphorylation and dephosphorylation of amino acid residues in the proteins.<sup>5</sup> It is noteworthy that formation of high-coordinate phosphoric intermediates is usually described as a key step in most enzyme catalytic mechanisms.<sup>6</sup>

It has been shown in our laboratory that *N*-phosphorylamino acids and peptides are chemically active species,<sup>7</sup> which might be related to the prebiotic synthesis of proteins and nucleotides and the phosphorylation or dephosphorylation of proteins.<sup>8</sup> An intramolecular pentacoordinate carboxylic–phosphoric mixed anhydride was proposed as the common intermediate for the reactions of *N*-phosphorylamino acids.<sup>9–10</sup> The pentacoordinate

(3) (a) Yoshida, H.; Watanabe, A.; Ihara, Y. *J. Biol. Chem.* **1999**, 274, 7368. (b) Shimizu, T.; Watanabe, A.; Ogawara, M.; Mori, H.; Shirasawa, T. *Arch. Biochem. Biophys.* **2000**, 381, 225.

(4) (a) Tyler-Cross, R.; Schirch, V. *J. Biol. Chem.* **1991**, 266, 22549. (b) Sandmeier, E.; Hunziker, P.; Kunz, B.; Sack, R.; Christen, P. *Biochem. Biophys. Res. Commun.* **1999**, 261, 578.

(5) Stock, J. B.; Ninfa, A. J.; Stock, A. M. *Microbiol. Rev.* **1989**, 53, 450.

(6) (a) Lee, Y. H.; Ogata, C.; James, W.; Levitt, D. G.; Sarma, R.; Banaszak, L. J.; Pilks, S. J. *Biochemistry* **1996**, 35, 6010. (b) Bernstein, B. E.; Machels, P. A. M.; Hol, W. G. J. *Nature* **1997**, 385, 275.

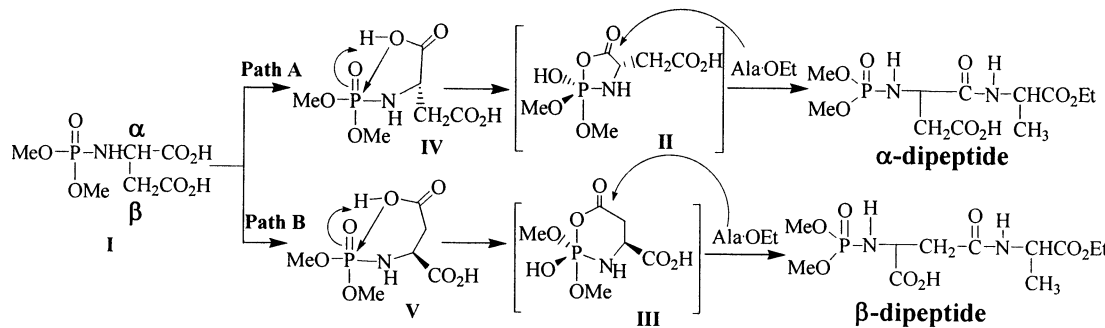
(7) (a) Xue, C. B.; Yin, Y. W.; Zhao, Y. F. *Tetrahedron Lett.* **1988**, 29, 1145. (b) Ma, X. B.; Zhao, Y. F. *J. Org. Chem.* **1989**, 54, 4005.

(8) (a) Zhao, Y. F.; Cao, P. S. *J. Biol. Phys.* **1994**, 20, 283. (b) Fu, H.; Li, Z. Z.; Zhao, Y. F.; Tu, G. Z. *J. Am. Chem. Soc.* **1999**, 121, 291.

\* To whom correspondence should be addressed. Fax: 86-10-62781695.

(1) (a) Seebach, D.; Matthews, J. L. *Chem. Commun.* **1997**, 21, 2015–2022. (b) Seebach, D.; Abele, S.; Gademann, K.; Jaun, B. *Angew. Chem., Int. Ed.* **1999**, 38, 1595–1597.

(2) (a) Herbert, L.; Wilfried, H. *Exp. Gerontol.* **2001**, 36, 1551. (b) Robinson, A. B.; Robinson, L. R. *Proc. Natl. Acad. Sci. U.S.A.* **1991**, 88, 8880.

**SCHEME 1. Possible Reaction Mechanism Involved in Formation of Pentacoordinate Phosphorane Intermediates from N-Phosphorylamino Acids**

phosphorane intermediates were trapped by using trimethylsilyl derivatives of  $\alpha$ -amino acids and  $O,O$ -phenylene phosphorochloridate reagents.<sup>10</sup> Furthermore, the formation of intermediates was the rate-determining step, and no intermediate was found for phosphoryl  $\beta$ -amino acids.

Previously, the activity difference between  $\alpha$ -COOH and  $\beta$ -COOH was studied by the ester exchange experiments and MNDO method.<sup>11</sup> However, it is very difficult to get the purified peptide because of the high and multifunctional reactivity of *N*-phosphorylamino acids under mild conditions. After careful separation, phosphoryl dipeptides were analyzed by NMR techniques, and Hartree-Fock (HF) and density functional theory (DFT) were carried out to study the mechanism of the formation of dipeptides in this paper.

## 2. Results and Discussions

**2.1. Analysis of Phosphoryl Peptide Esters by NMR Techniques.** When *N*-( $O,O$ -diisopropyl)phosphoryl-L- $\alpha$ -aspartylalanine (DIPP-Asp) and ethyl alanine ester (Ala-OEt) were incubated in chloroform for 1 h without any coupling reagents, the dipeptide DIPP-Asp-Ala-OEt was found (Scheme 1), as evidenced by  $^{31}$ P NMR and ESI mass spectra ( $M_w$  396). Since *N*-phosphorylamino acid and peptide are active in solution, the yield of phosphoryl dipeptide was very low. But it is not certain whether the reaction goes through path A, path B, or both. To address this question, the reaction mixture was separated on a silica gel column by gradient elution. After separation, phosphorylaspartic acid was removed. The desired portion was analyzed to determine which of the carboxylic groups in DIPP-Asp is involved in the reaction.

The assignments of  $^1$ H and  $^{13}$ C resonances in the phosphoryl aspartyl dipeptide ester are based on the 2D COSY, NOESY,  $^1$ H- $^{13}$ C HMQC,  $^1$ H- $^{13}$ C HMBC, and 1D  $^{13}$ C spectra. The results are shown in Table 1. The data are consistent with the previous work by Xue et al.<sup>12</sup> The resonances of the carbonyl groups are shown in Figure 1. In the 1D  $^{13}$ C spectrum (Figure 1a), the peak at around

**TABLE 1.  $^1$ H and  $^{13}$ C NMR Data for Ethyl *N*-( $O,O$ -Diisopropyl)phosphoryl-L- $\alpha$ -aspartylalanine<sup>a</sup>**

group	residue	$^1$ H ( $\delta$ )	mult	$J$ (Hz)	$^{13}$ C ( $\delta$ )
NH	Ala	7.37	d	7.97	
C <sup>a</sup> O	Asp				171.988 171.911
CO	Ala				173.2
C <sup>b</sup> OOH	Asp	6.2–6.6	broad		175.1
NH	Asp	5.11	t	$^2J = 11.7$ , $^3J = 5.9$ <sup>b</sup>	
CH	Ala	4.56	m		49.1
CH	Pr <sup>i</sup>	4.56	m	6.60	73.0
CH <sub>2</sub>	Et	4.18	q	7.10	62.0
C <sup>a</sup> H	Asp	3.79	m		52.2
C <sup>b</sup> H	Asp	3.27	q	$^2J = 17.8$ , $^3J = 2.8$ <sup>c</sup>	37.244
	Asp	2.68	q	$^2J = 17.8$ , $^3J = 5.0$ <sup>c</sup>	37.218
CH <sub>3</sub>	Ala	1.42	d	7.97	18.8
CH <sub>3</sub>	Pr <sup>i</sup>	1.33	q	6.60	24.3
CH <sub>3</sub>	Et	1.26	t	7.10	14.8

<sup>a</sup>  $^{13}$ C NMR was  $^1$ H decoupled. <sup>b</sup>  $^2J$  is  $^2J_{\text{HNP}}$ ;  $^3J$  is  $^3J_{\text{HNO}}$ . <sup>c</sup>  $^2J$  is  $^2J_{\beta\beta}$  of C<sup>b</sup>H groups in Asp residue;  $^3J$  is  $^3J_{\beta\alpha}$  of C<sup>b</sup>H and C<sup>a</sup>H groups in Asp residue.

171.9 ppm is assigned to the  $\alpha$  carbonyl group of the aspartic residue, for it is split by the phosphorus nucleus. In the HMBC spectrum (Figure 1b), the peak at 173.2 ppm shows long-range  $^1$ H- $^{13}$ C connectivity with CH (Ala, 4.56 ppm), CH<sub>3</sub> (Ala, 1.42 ppm), and CH<sub>2</sub> (Et, 4.18 ppm). Thus, the peak is assigned to the carbonyl group of the Ala residue. In a similar way, the peak at 175.1 ppm is assigned to the  $\beta$  carbonyl group of the aspartic residue.

The key data to establish the nature of the Asp-Ala peptide linkage<sup>13</sup> were obtained from NOESY, HMBC, and  $^{13}$ C NMR spectra (Figures 1 and 2). The NOESY spectrum (Figure 2) shows strong NOE intensity between C<sup>a</sup>H (Asp, 3.79 ppm) and NH (Ala, 7.37 ppm) ( $d_{\alpha\text{N}}$ ), NH (Asp, 5.11 ppm), and NH (Ala, 7.37 ppm) ( $d_{\text{NN}}$ ), while those of the two C<sup>b</sup>H (Asp, 2.68 and 3.27 ppm) and NH (Ala, 7.37 ppm) ( $d_{\beta\text{N}}$ ) are extremely weak. The low intensities of  $d_{\beta\text{N}}$  indicate that the inter-hydrogen distances between the two C<sup>b</sup>H (Asp) and the NH (Ala) are near the upper limits of NOESY inter-hydrogen distance (4–6 Å). The strong intensities of  $d_{\text{NN}}$  and  $d_{\alpha\text{N}}$  show that NH (Ala) is very close to C<sup>a</sup>H(Asp) and NH(Asp). This observation is consistent with a normal  $\alpha$ -linked peptide backbone because structural constraints force at least one of the two distances ( $d_{\alpha\text{N}}$ ,  $d_{\text{NN}}$ ) to be less than 3 Å.<sup>14</sup> From the results of ab initio calculations on the phosphoryl

(9) (a) Zhong, R. G.; Zhao, Y. F.; Dai, Q. H. *Chin. Sci. Bull.* **1998**, 43, 917. (b) Ramirez, F.; Marecek, J. F.; Okazaki, H. *J. Am. Chem. Soc.* **1976**, 98, 5310.

(10) (a) Wang, Q.; Zhao, Y. F.; An, F. L.; Mao, Y. Q.; Wang, Q. Z. *Sci. China, Ser. B* **1995**, 25, 683. (b) Fu, H.; Tu, G. Z.; Li, Z. L.; Zhao, Y. F.; Zhang, R. Q. *J. Chem. Soc., Perkin Trans. 1* **1997**, 2021.

(11) Chen, Z. Z.; Tan, B.; Li, Y. M.; Zhao, Y. F. *Int. J. Quantum Chem.* **2001**, 83, 41.

(12) Xue, C. B.; Yin, Y. W.; Zhao, Y. F.; *J. Chem. Soc., Perkin Trans. 2* **1990**, 431.

(13) Chazin, W. J.; Kördel, J.; Thulin, E.; Hofmann, T.; Drakenberg, T.; Försén, S. *Biochemistry* **1989**, 28, 8646.

(14) Billeter, M.; Braun, W.; Wüthrich, K. *J. Mol. Chem.* **1982**, 155, 321.

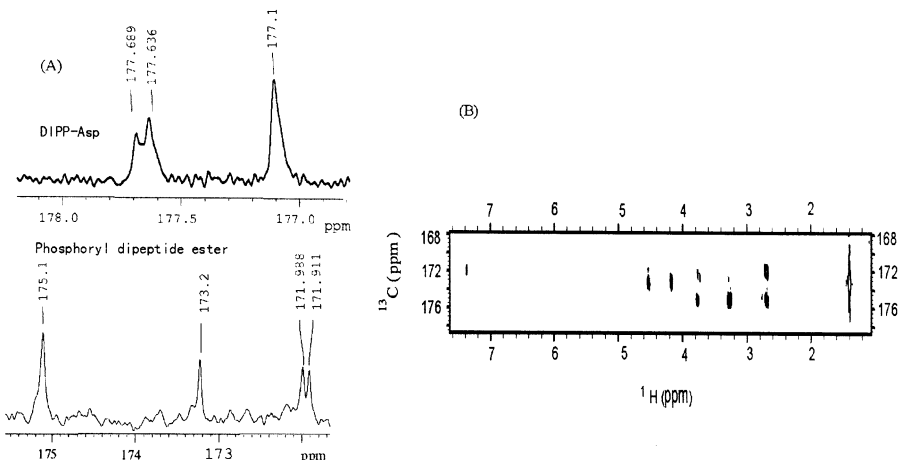
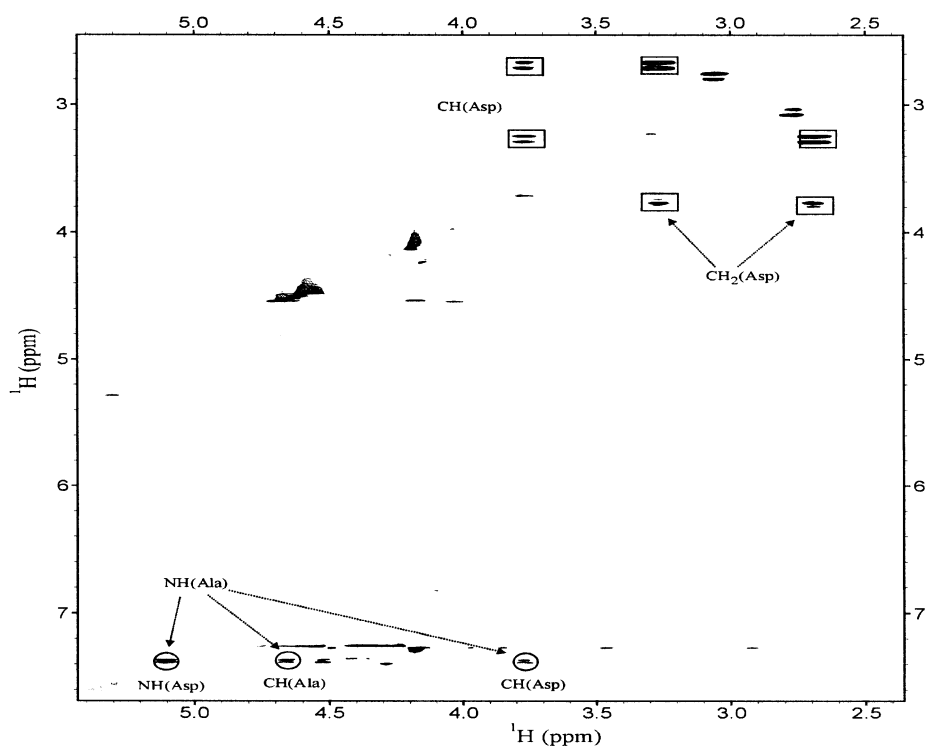


**FIGURE 1.** (A) <sup>13</sup>C spectra of carbonyl groups in DIPP-Asp and phosphoryl dipeptide ester. (B) HMBC spectra in carbonyl group area. For the assignment of the peaks, see the text for details.



$\alpha$ -dipeptide ester at the HF/6-31G\*\* level, the distances between C<sup>a</sup>H (Asp) and NH (Ala) and between C<sup>b</sup>H (Asp) and NH (Ala) are 2.383, 3.414, and 3.917 Å, respectively. The corresponding distances are 4.316, 2.210, and 3.326 Å for the  $\beta$ -dipeptide ester, respectively. Thus, on the basis of the NOESY spectrum and the results of calculations, the dipeptide ester formed should be an  $\alpha$ -dipeptide ester.

In the HMBC spectrum (Figure 1b), a strong sequential connectivity between the NH (Ala) and the  $\alpha$  carbonyl group of Asp residue was observed, while there was no cross-peak observed between the NH (Ala) and  $\beta$  carbonyl group of the Asp residue. The data give rise to an unambiguous conclusion that the phosphoryl aspartyl peptide ester must be an  $\alpha$ -peptide, not a  $\beta$ -peptide. This

result is also supported by the following facts. Generally, the carbonyl group in amide moiety had lower chemical shift than that in the free carboxylic group. For DIPP-Asp, the <sup>13</sup>C chemical shifts of the  $\alpha$  and  $\beta$  carbonyl groups were 177.6 (doublet) and 177.1 ppm (Figure 1a, upper panel), respectively. Compared to the <sup>13</sup>C chemical shift of the  $\beta$  carbonyl group, only the <sup>13</sup>C chemical shift of the  $\alpha$  carbonyl group decreased greatly in the phosphoryl aspartyl dipeptide ester, which indicates change of the bonding of the  $\alpha$  carbonyl group.

From the above results, we conclude that the phosphoryl dipeptide ester formed is solely an  $\alpha$ -dipeptide ester.

**2.2. Theoretical Calculations.** *N*-Phosphorylaspartic acid has both  $\alpha$ -COOH and  $\beta$ -COOH. But it is not known

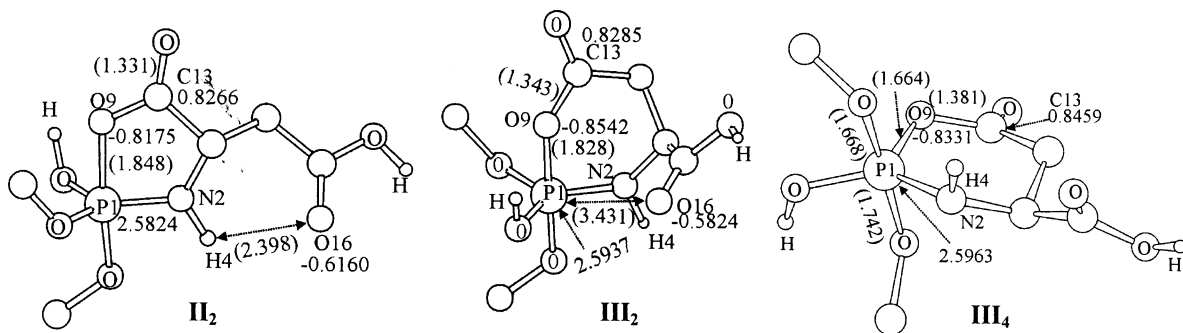


**FIGURE 3.** Optimized structures of **II**<sub>2</sub>, **III**<sub>2</sub>, and **III**<sub>4</sub> at the B3LYP/6-31G\*\* level. The NBO atomic charges and the distances (in parentheses, Å) are shown.

theoretically which carboxylic group,  $\alpha$  (path A) or  $\beta$  (path B), is involved in the formation of the pentacoordinate phosphorane intermediates (Scheme 1).

The model molecule DMP-Asp (**I**, DMP = *N*-dimethylphosphoryl) is constructed according to the crystal structure of *N*-diisopropylphosphorylalanine (DIPP = *N*-diisopropylphosphoryl).<sup>15</sup> For **I** at the B3LYP/6-31G\*\* level, the NBO positive charge of the proton in  $\alpha$ -CO<sub>2</sub>H is about 0.0027 larger than that of the proton in  $\beta$ -CO<sub>2</sub>H. Hence, a proton might be easier to transfer from  $\alpha$ -CO<sub>2</sub>H than from  $\beta$ -CO<sub>2</sub>H. Meanwhile, the  $\alpha$ -CO<sub>2</sub><sup>-</sup> anion derived from **I** is 18.51 kJ/mol more stable than the  $\beta$ -CO<sub>2</sub><sup>-</sup> anion at the HF/6-31G\*\* level, and the  $\beta$ -CO<sub>2</sub><sup>-</sup> anion would be converted to the  $\alpha$ -CO<sub>2</sub><sup>-</sup> anion at the B3LYP/6-31G\*\* level. This favors the nucleophilic attack of  $\alpha$ -COOH group on the phosphorus atom. As a result, the formation of the pentacoordinate phosphorane intermediates from the  $\alpha$ -COOH group might become easier.

**Comparison of Pentacoordinate Phosphorane Intermediates **II** and **III**.** There are two types of possible pentacoordinate phosphorane intermediates: **II**, containing a five-membered ring formed by  $\alpha$ -COOH; and **III**, containing a six-membered ring by  $\beta$ -COOH (Scheme 1). Pentacoordinate phosphorane intermediates **II** and **III** prefer tbp (trigonal bipyramidal) configurations because of the lack of bicyclic rings and an electronic imbalance of the five different ligands.<sup>16</sup> There are six positional isomers with the ring in an apical-equatorial spanning arrangement for **II** and **III**. These isomers can be classified according to the position of the P–N bond: equatorial or apical. From the calculations by the MNDO method<sup>11</sup> and the DFT method (for DMP-Ala), the former is more stable than the latter because of the high apicophilicity of the oxygen atom. Furthermore, experiments have shown that the P–O bond of the anhydride P–O–CO moiety is in the apical position.<sup>10b</sup> Thus, those positional isomers with a P–N bond in the apical positions are not further considered in this paper.

Three isomers (**II**<sub>1</sub>–**II**<sub>3</sub>) for intermediate **II** are considered here, while six isomers (**III**<sub>1</sub>–**III**<sub>6</sub>) are taken into account for intermediate **III** because the arrangement of the six-membered ring might adopt apical-equatorial or diequatorial spannings.<sup>17</sup> To determine which isomers

**TABLE 2. Relative Energy (RE) of Pentacoordinate Phosphorane Intermediates at the HF/6-31G\*\* Level**

compd <sup>a</sup>	RE (kJ/mol)	compd	RE (kJ/mol)
<b>II</b> <sub>1</sub>	48.92	<b>III</b> <sub>3</sub>	99.87
<b>II</b> <sub>2</sub>	32.74	<b>III</b> <sub>4</sub>	161.88
<b>II</b> <sub>3</sub>	47.19	<b>III</b> <sub>5</sub>	170.87
<b>III</b> <sub>1</sub>	104.51	<b>III</b> <sub>6</sub>	171.52
<b>III</b> <sub>2</sub>	85.29		

<sup>a</sup> The relative energies (RE) refer to the energies relative to **I**. **II** and **III** stand for intermediates containing five- or six-membered rings, respectively. The hydroxyl group is on the ring plane for **1**, **4**; on the same side of the residual carboxylic group for the plane for **2**, **5**; and on the different side for **3**, **6**.

are most stable, the nine isomers are optimized at the HF/6-31G\*\* level and their relative energies are listed in Table 2. Isomer **II**<sub>2</sub> is most stable among intermediates **II**. For the intermediates **III**, isomer **III**<sub>2</sub> has the lowest energy and isomer **III**<sub>4</sub> is most stable among isomers with six-membered ring in diequatorial spanning arrangement. For both types of intermediates, the most stable isomers are those in which the hydroxyl group is in an equatorial position and the hydroxyl group and the residual COOH are on the same side of the ring. This is because the equatorial positioning of the less bulky hydroxyl group reduces the steric hindrance of the phosphorus atom and thus makes those isomers more stable.

The optimized geometries of **II**<sub>2</sub>, **III**<sub>2</sub>, and **III**<sub>4</sub> at the B3LYP/6-31G\*\* level are depicted in Figure 3. It can be seen that the geometries of **II** and **III** are twisted trigonal bipyramids, which is in agreement with that predicted in the reference.<sup>18</sup> For **II**<sub>2</sub>, the atoms in the five-membered ring are almost coplanar. For **III**<sub>2</sub>, the six-membered ring is in a boat form, while the six-membered ring is in a chair form for isomer **III**<sub>4</sub>. Comparison of the three isomers reveals major difference in both conformations (Figure 3) and thermodynamic parameters (Table 3). The relatively longer bond of P–O and the larger distance between the phosphorus and O16 atoms in isomer **II**<sub>2</sub> than those in the isomers of **III** indicate the phosphorus atom is less crowded in **II**<sub>2</sub>. Also noteworthy is the formation of an intramolecular hydrogen bond N2–H4···O16 in **II**<sub>2</sub>. The shorter bond O9–C13 and the less absolute NBO charges of P, O9, and C13 atoms in isomer

(15) Xue, C. B.; Yin, Y. W.; Liu, Y. M.; Zhu, N. J.; Zhao, Y. F. *Phosphorus, Sulfur Silicon Relat. Elem.* **1989**, *42*, 149.

(16) Emsley, J.; Hall, D. *The Chemistry of Phosphorus: Environmental, Organic, Inorganic, Biochemical and Spectroscopic Aspects*; Harper & Row Ltd: London, 1976; Chapter 2.

(17) Corbridge, D. E. C. *Phosphorus: an Outline of Its Chemistry, Biochemistry and Technology*, 5th ed; Elsevier: New York, 1995; Chapter 13.

(18) Holmes, R. R. *J. Am. Chem. Soc.* **1975**, *97*, 5379.

**TABLE 3. Relative Energy (RE) and Strain Energy of Key Intermediates and Transition States**

RE (kJ/mol)	HF/6-31G**	$\Delta H^a$	$\Delta G^a$	strain energy <sup>a</sup>	energy in solvent <sup>b</sup>	single-point energy <sup>c</sup>
<b>II<sub>2</sub></b>	32.74	12.03	20.57	-90.87	3.13	22.78
<b>IV</b>	93.94	55.09	61.41		46.53	73.21
<b>III<sub>2</sub></b>	85.29	60.24	68.73	5.26	51.44	70.98
<b>V</b>	120.81	100.83	111.25		88.55	117.78
<b>III<sub>4</sub></b>	161.88	121.35	134.89	63.50	112.82	137.63
$\Delta E(\text{III}_2 - \text{II}_2)$	52.55	48.21	48.16		48.31	48.20

<sup>a</sup>  $\Delta H$  and  $\Delta G$  strain energies were calculated at the B3LYP/6-31G\*\* level. For  $\Delta H$  and  $\Delta G$ , zero-point correction and thermal correction were considered. Only zero-point correction is considered in the strain energy. <sup>b</sup> The energy was calculated at the B3LYP/6-31G\*\* level with  $\text{CHCl}_3$  ( $\epsilon = 4.9$ ) as solvent. <sup>c</sup> The single-point energy was calculated at the B3LYP/6-311+G\*\*//B3LYP/6-31G\*\* level (not considering the ZPE, thermal correction, and solvation).

**II<sub>2</sub>** mean that **II<sub>2</sub>** is less active than the isomers of **III**. So the isomer **II<sub>2</sub>** containing a five-membered ring is about 48.21 kJ/mol in energy lower than **III<sub>2</sub>** with a six-membered ring thermodynamically. Isomer **III<sub>2</sub>** is about 61.11 kJ/mol lower than **III<sub>4</sub>** at the B3LYP/6-31G\*\* level. The arrangements of the two six-membered rings also differ greatly in the two isomers of **III**. In **III<sub>4</sub>**, the angle of N2-P-O9 is 109.9°, which is smaller than the standard angle of tbp configuration (120°). It implies that the ring in isomer **III<sub>4</sub>** is more crowded than that in isomer **III<sub>2</sub>**. The shorter bond of P-O9 in **III<sub>4</sub>** makes it even more crowded than **III<sub>2</sub>**. Thus, the location of the six-membered ring in the apical-equatorial position of a trigonal bipyramidal is the most common geometry. These results are also consistent with previous experiments and theoretical computations.<sup>17</sup>

To understand the relative stabilities of these intermediates, the strain energies are calculated from the homodesmotic reactions<sup>19</sup> at the B3LYP/6-31G\*\* level (Table 3). The calculated strain energies indicate that **II<sub>2</sub>** is less strained than **III<sub>2</sub>**, which is less strained than **III<sub>4</sub>**. This may be attributed to the high p- and d-characters of the P-O9 bond and the stabilization energy contributed by the  $\sigma$ - $\sigma^*$  interaction in the ring.<sup>20</sup> The p- and d-characters of the hybrid orbitals for phosphorus atom in the P-O9 bond increase in the following order:  $\text{sp}^{3.64}\text{d}^{0.42}$  (**III<sub>4</sub>**),  $\text{sp}^{3.45}\text{d}^{2.58}$  (**III<sub>2</sub>**), and  $\text{sp}^{3.54}\text{d}^{2.75}$  (**II<sub>2</sub>**). The sigma-sigma\* interactions between P-O9 bond and P-N2  $\sigma^*$ , P-N2 bond and P-O9  $\sigma^*$  in **II<sub>2</sub>** are 90.75 and 164.43 kJ/mol, respectively. The corresponding values are 86.94 and 155.56 kJ/mol in **III<sub>2</sub>**, respectively, and are less than 2.1 kJ/mol in **III<sub>4</sub>**. This order is in agreement with the energy order of these intermediates.

**Substitution Groups on the Phosphorus Atom.** Since phosphorylamino acids with isopropyl groups on the phosphorus atom are more stable at rt, they have been widely used experimentally in biomimetic reactions.<sup>8,10,11,21</sup> But since it is computationally more time demanding for the large isopropyl group than for the methyl group and the substitution groups on the phosphorus atom are not directly involved in the reaction, the previous calculations are simplified by replacing isopropyl groups with methyl groups. To determine whether such replacement is reasonable or not, the geometries of **I'**,

(19) George, P.; Trachtman, M.; Bock, C. W.; Brett, A. M. *Tetrahedron* **1976**, *32*, 317.

(20) (a) Inagaki, S.; Ishitani, Y.; Kakefu, T. *J. Am. Chem. Soc.* **1994**, *116*, 5954. (b) Inagaki, S.; Yoshikawa, K.; Hayano, Y. *J. Am. Chem. Soc.* **1993**, *115*, 3706. (c) Inagaki, S.; Goto, N.; Yoshikawa, K. *J. Am. Chem. Soc.* **1991**, *113*, 7144.

(21) Li, Y. M.; Zhang, D. Q.; Zhang, H. W.; Ji, G. J.; Zhao, Y. F. *Bioorg. Chem.* **1992**, *20*, 285.

**TABLE 4. Relative Energy (RE) of Pentacoordinate Phosphorane Intermediates for the Isopropyl Group<sup>a</sup>**

RE (kJ/mol)	HF/6-31G**	$\Delta H$	single-point energy
<b>II'2</b>	30.16	11.72	18.56
<b>III'2</b>	84.06	61.88	68.60
$\Delta E(\text{III}'_2 - \text{II}'_2)$	53.90	50.16	50.04

<sup>a</sup>  $\Delta H$  and the single-point energy are same as in Table 3.

**II'2**, and **III'2** with isopropyl groups on the phosphorus atom are optimized by ab initio and DFT calculations, with relative energies shown in Table 4.

At the B3LYP/6-31G\*\* and B3LYP/6-311+G\*\*//B3LYP/6-31G\*\* levels, the relative energies of **II'2** and **III'2** are almost the same as those with methyl groups (Table 3 and Table 4). The geometries of **I'**, **II'2**, and **III'2** are close to those with methyl groups in the corresponding levels. The relative stability of **II'2** and **III'2**, i.e., the energy difference  $\Delta E(\text{III}'_2 - \text{II}'_2)$ , is also comparable with the relative stability of **II<sub>2</sub>** and **III<sub>2</sub>**,  $\Delta E(\text{III}_2 - \text{II}_2)$ . Thus, the model substituting the isopropyl groups with the methyl groups for calculations is reasonable.

**Geometries of the Transition States and the Possible Mechanisms.** Isomers **II<sub>2</sub>** and **III<sub>2</sub>**, the most stable isomers among intermediates **II** and **III**, are selected to search for transition states. The transition states **IV** and **V** are fully optimized by the STQN<sup>22</sup> method at the HF/6-31G\*\* and B3LYP/6-31G\*\* level, with their geometry at the B3LYP/6-31G\*\* level shown in Figure 4. The results of frequency calculations reveal that **IV** and **V** each have only one imaginary frequency at 272.75i and 196.63i  $\text{cm}^{-1}$ , respectively. The vibrational modes corresponding to the imaginary vibrational frequencies of **IV** and **V** show that the optimized structures are the true transition states with one imaginary frequency corresponding to the proton H10 transfer to O3 atom and the bond P-O9 formation. Thus, the proton transfer and the bond formation of P-O9 cooperate in the formation of the intermediates. According to Figure 4, transition states **IV** or **V** contain a hydrogen-bond-bridge moiety O3-H10-O9. NBO analysis reveals that the bonds of H10-O3 and P-O9 are partially formed in the transition states **IV** and **V**. A hydrogen bond N2-H4 $\cdots$ O16 is formed in **IV**, but not in **V**, making transition state **IV** more stable. The shorter bond length of P-O9 and the proximity of O16 atom to the phosphorus atom in **V** make it more crowded than that in **IV**. The less NBO atomic absolute charges of O9 and H10 indicate that **IV**

(22) Peng, C.; Ayala, P. Y.; Schlegel, H. B.; Frisch, M. J. *J. Comput. Chem.* **1996**, *17*, 49.

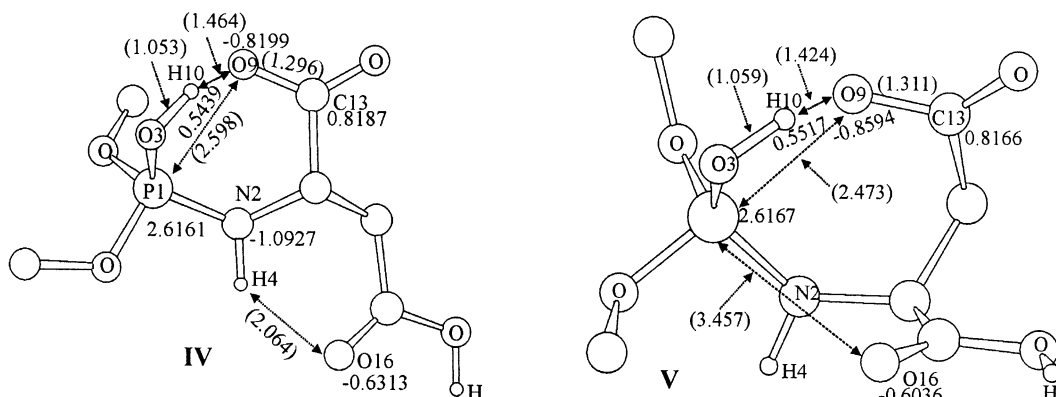


**FIGURE 4.** Optimized structures of **IV** and **V** at the B3LYP/6-31G\*\* level. The NBO atomic charges and the distances (in parentheses, Å) are shown.

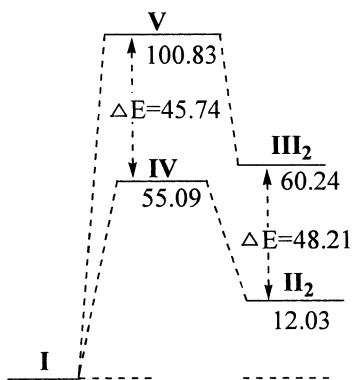


**FIGURE 5.** Energy ( $\Delta H$ , kJ/mol) profile for reactant, intermediates, and transition states at the B3LYP/6-31G\*\* level.

is less active than **V**. As a result, the energy of **V** is 45.74 kJ/mol higher than that of **IV** (Figure 5).

Experimentally, the peptide formation of *N*-phosphorylamino acids proceeds in CHCl<sub>3</sub>. The solvent effects are calculated by using the PCM model<sup>23</sup> at the B3LYP/6-31G\*\* level. The energies of the above-mentioned intermediates and transition states in CHCl<sub>3</sub> are listed in Table 3. The energy barrier in forming intermediate **II**<sub>2</sub> (path A) is 42.02 kJ·mol<sup>-1</sup> lower than that in forming **III**<sub>2</sub> (path B). For both paths A and B, the solvent effect largely promotes the positive reactions. This is because the dipole moments of the transition states are larger than those of the pentacoordinate phosphorane intermediates, which are larger than the phosphorylamino acid. The much lower energy barrier in forming the five-membered ring intermediate **II**<sub>2</sub> indicates that the reaction via path A will happen far more easily under mild conditions than that via path B.

### 3. Summary and Conclusion

Phosphoryl dipeptide can be formed directly from phosphorylaspartic acid without coupling reagents. A detailed analysis of the chemical shifts and coupling constants of the dipeptide by NMR techniques indicate that the phosphoryl peptide formed linkage is an  $\alpha$ -pep-

tide, not a  $\beta$ -peptide. The results of the calculations imply that the formation of pentacoordinate phosphorane intermediates follows path A by the participation of  $\alpha$ -COOH and that the reaction could occur under mild conditions without any additional activating reagent, as confirmed in the experiments. The activity of  $\alpha$ -COOH is higher than  $\beta$ -COOH after *N*-phosphorylation, and only the  $\alpha$ -COOH group is involved in the reactions. This result is consistent with the fact that only  $\alpha$ -unprotected amino acids have biomimetic reactivities.<sup>21</sup> These might be helpful in understanding the question as to why nature chose  $\alpha$ -amino acids, not  $\beta$ -amino acids, as protein backbone.

### 4. Experimental and Computational Methods

**4.1. Apparatus.** The ESI mass spectra were obtained on an ion-trap mass spectrometer. The <sup>31</sup>P NMR spectra were acquired 200 MHz spectrometer with 85% phosphoric acid as the external reference. All <sup>1</sup>H, <sup>13</sup>C NMR, and 2D NMR spectra were acquired at 298 K on a spectrometer equipped with XYZ gradients, except when otherwise specified. TMS was added for <sup>1</sup>H referencing, and <sup>13</sup>C chemical shifts were indirectly referenced to TMS.<sup>24</sup> Standard Bruker pulse programs were used for the acquisition of DQF-COSY, HMBC, HMQC, and NOESY spectra (see the Supporting Information). Data were either processed with Xwin-NMR or Felix 98.0. All quantum chemistry calculations were carried out with Gaussian 98 software<sup>25</sup> on a SGI Power Challenger R12000 workstation. All molecular modeling was performed with the SYBYL6.7 software package (Tripos Inc., St. Louis, MO, 2000).

**4.2. Preparation of Samples.** *N*-(*O*,*O*'-Diisopropyl)phosphoryl-L-aspartic acid (DIPP-Asp) was prepared according to previously published protocol.<sup>21</sup>

**Formation and Isolation of the Phosphoryl Dipeptide Ester by Self-Activation of DIPP-Asp.** A 1.00 g sample of DIPP-Asp was dissolved in 16 mL of CHCl<sub>3</sub>. Then 0.40 g of triethylamine and 0.57 g of HCl-Ala-OEt were added, and the

(24) Bax, A.; Subramanian, S. *J. Magn. Reson.* **1986**, 67, 565.

(25) Frisch, M. J.; Trucks, G. W.; Schlegel, H. B.; Scuseria, G. E.; Robb, M. A.; Cheeseman, J. R.; Zakrzewski, V. G.; Montgomery, J. A., Jr.; Stratmann, R. E.; Burant, J. C.; Dapprich, S.; Millam, J. M.; Daniels, A. D.; Kudin, K. N.; Strain, M. C.; Farkas, O.; Tomasi, J.; Barone, V.; Cossi, M.; Cammi, R.; Mennucci, B.; Pomelli, C.; Adamo, C.; Clifford, S.; Ochterski, J.; Petersson, G. A.; Ayala, P. Y.; Cui, Q.; Morokuma, K.; Malick, D. K.; Rabuck, A. D.; Raghavachari, K.; Foresman, J. B.; Cioslowski, J.; Ortiz, J. V.; Baboul, A. G.; Stefanov, B. B.; Liu, G.; Liashenko, A.; Piskorz, P.; Komaromi, I.; Gomperts, R.; Martin, R. L.; Fox, D. J.; Keith, T.; Al-Laham, M. A.; Peng, C. Y.; Nanayakkara, A.; Challacombe, M.; Gill, P. M. W.; Johnson, B.; Chen, W.; Wong, M. W.; Andres, J. L.; Gonzalez, C.; Head-Gordon, M.; Replogle, E. S.; Pople, J. A. *Gaussian98*, revision A.9; Gaussian, Inc.; Pittsburgh, PA, 1998.

(23) (a) Miertus, S.; Scrocco, E.; Tomasi, J. *Chem. Phys.* **1981**, 55, 117. (b) Miertus, S.; Tomasi, J. *Chem. Phys.* **1982**, 65, 239. (c) Tomasi, J.; Persico, M. *Chem. Rev.* **1994**, 94, 2027.

mixture was incubated at 40 °C for 1 h or more and monitored with  $^{31}\text{P}$  NMR and ESI-MS. After the incubation, the solvent was evaporated and the residue was dissolved in water. The pH of the aqueous solution was adjusted to 9.0 with 1 M NaOH. The reaction mixture was then washed with ethyl acetate, acidified to pH = 3.0 with dilute HCl, extracted with a mixed solvent of *tert*-butyl alcohol and ethyl acetate (2:3, vol/vol), and finally dried with MgSO<sub>4</sub>. The phosphoryl dipeptide was isolated on silica gel column by gradient elution. The eluting solvents consisted of petroleum ether, chloroform, and methanol. Total yield was 5–6%.

**4.3. Modeling and Computational Details.** *N*-Dimethylphosphoryl-L-aspartic acid **I** was taken as the model reactant, and the possible mechanisms are shown in Scheme 1. One possible mechanism is through pentacoordinate phosphorane intermediates **II** by the attack of  $\alpha$ -COOH (path A). The other is through **III** by the attack of  $\beta$ -COOH (path B).

The geometry for reactant and intermediates was optimized at the HF/6-31G\*\* and B3LYP/6-31G\*\* level.<sup>26</sup> The transition states **IV** and **V** were found with synchronous transit-guided quasi-Newton (STQN) methods.<sup>22</sup> Natural bond orbital (NBO)

analysis<sup>27</sup> and frequency calculations were performed at the same level for each optimized structure. All the energy at the B3LYP/6-31G\*\* level was corrected by zero-point vibrational energy (ZPE). The single-point energies were performed at the B3LYP/6-311+G\*\*/B3LYP/6-31G\*\* level. Finally, the geometries determined at the B3LYP/6-31G\*\* level were employed to perform the calculations of the solvent effects by the PCM model<sup>23</sup> in CHCl<sub>3</sub> solution. The calculated free energy in solution was taken as the energy in the gas phase (including ZPE) plus the solvent shift. The relative energies (RE) in this work refer to the energies relative to **I**.

**Acknowledgment.** We thank the Chinese National Natural Science Foundation (No. 20072023 and NS-FCBIC 20320130046) and Tsinghua University for the financial support.

**Supporting Information Available:** NMR techniques, NMR spectra, geometries, and Cartesian matrixes of optimized structures. This material is available free of charge via the Internet at <http://pubs.acs.org>.

JO0300082

(26) (a) Becke, A. D. *J. Chem. Phys.* **1993**, *93*, 5648. (b) Wu, Y. D.; David, K. W. L. *J. Am. Chem. Soc.* **1995**, *117*, 11327.

(27) Glendening, E. D.; Reed, A. E.; Carpenter, J. E.; Weinhold, F. *NBO Version 3.1*.